



Research Article

Mathematical analysis of fractional order Covid 19 epidemic model

Pınar AÇIKGÖZ¹, Mehmet MERDAN^{1,*}

¹Department of Mathematical Engineering, Faculty of Engineering and Natural Science, Gümüşhane University, Gümüşhane, 29100, Türkiye

ARTICLE INFO

Article history

Received: 24 May 2024

Revised: 03 July 2024

Accepted: 04 October 2024

Keywords:

Conformable Derivative;
Conformable Differential
Transformation; Covid 19
Model; Variational Iteration
Method

ABSTRACT

This article aims to examine the dynamics of the fractional epidemic model of covid 19. The model in question incorporates the notion of a compatible derivative. Given their consistent and worldwide characteristics, fractional derivatives are presently employed to address numerous practical issues. In addition, we employ two numerical techniques, namely the conformal differential transform and the variational iteration approach, to provide an approximate solution for the given model. The research closes by providing an in-depth analysis and visually representing the numerical findings. Furthermore, it has been demonstrated that the solution obtained is convergent.

Cite this article as: Açıkgöz P, Merdan M. Mathematical analysis of fractional order Covid 19 epidemic model. Sigma J Eng Nat Sci 2025;43(5):1720–1732.

INTRODUCTION

Epidemiology, also known as the “science of epidemics,” is a crucial discipline within the subject of public health. Epidemiology, commonly referred to as “epidemia,” is a field of study that examines the causative elements behind the occurrence and transmission of diseases within a specific timeframe and setting. Mathematical epidemiology has become a valuable scientific discipline for assessing the occurrence and death rates of epidemics, as well as identifying their underlying causes.

Epidemic disease models are a crucial component of contemporary mathematical modeling investigations. Several renowned organizations, such as the World Health Organization, the Centre for the Mathematical Modeling of Infectious Disease in England, and the BC Center for

Disease Control in Canada, engage in comprehensive research on disease modeling.

Mathematical models are employed across various fields such as biology, chemistry, psychology, and economics to enhance our understanding of real-world phenomena. Financial models often use stochastic equations, while ordinary differential equation systems are essential for forecasting the progression of infectious diseases. It is important to highlight the application of fractional analysis in studying the history of the event. This is because the current trend in mathematical modeling involves utilizing different types of fractional derivatives and solution methods to accurately, approximately, or numerically solve the system under investigation.

Compartment models for epidemiology are models that look at the kinetics of transmission and have been explored

*Corresponding author.

*E-mail address: mehmetmerdan@gmail.com

This paper was recommended for publication in revised form by
Editor-in-Chief Ahmet Selim Dalkilic



since the early 1900s [1-3]. These models have been used to generate pretty accurate estimates for many [4-6] and are still in use today for the Covid-19 [7-8]. Compartment models establish discrete divisions, known as compartments, within a society that is isolated or self-contained. Each compartment is designated by a capital letter. For example, the variable S represents the total number of individuals who are at risk of infection. The variable E represents the total number of individuals who are infected but not yet contagious. The variable I represents the total number of individuals who are infected and capable of spreading the infection. The variable R represents the total number of individuals who have recovered from the infection. The concept derives its name from the compartments, which are named after the specific disease-related states of individuals. The SIR model, sometimes referred to as the classical compartmental model, can be employed to develop new models for a wide range of diseases and situations. The SEIR model incorporates an edible compartment E (exposed) to represent the stage when a patient has been exposed to the disease but has not yet developed active symptoms in the body. Furthermore, the integration of different situations allows for the creation of epidemic illness models that encompass a range of compartments, including SIS, SEIR, SEIRS, and MSEIR.

They have formulated the model with five compartments. The mentioned model is given by:

$$\begin{aligned}\frac{dS}{dt} &= \Lambda - \phi_c IS - \mu S + v_3 R, \\ \frac{dE}{dt} &= \phi_c IS - (\sigma + \mu)E, \\ \frac{dI}{dt} &= \sigma E - (\alpha + v_2 + \delta + \mu)I + v_1 R, \\ \frac{dQ}{dt} &= \alpha I - (\theta + \mu)Q \\ \frac{dR}{dt} &= \theta Q - (v_1 + v_3 + \mu)R + v_2 I\end{aligned}\quad (1)$$

In this section, we present a mathematical system for the population at the time of COVID-19 and divide it into five parts [9]. S is susceptible, E is exposed, I is infected, Q is quarantined, and R is recovered.

It is important to mention that scholars have previously and now utilized integer derivatives to simulate a diverse array of biological and physical phenomena. Fractional mathematics has gained significant attention in the scientific world in the past two decades due to its importance. Mathematicians have diligently endeavored to formulate and analyze a diverse array of biological phenomena by employing fractional derivatives. Utilizing fractional derivatives offers numerous benefits. The Caputo and Riemann-Liouville definitions of fractional derivatives have nonlocal characteristics, such as the ability to retain information from the past and predict future behavior. It is important to

remark that the aforesaid topic is being more and more utilized in engineering and research domains such as optics, signal processing, viscoelasticity, fluid mechanics, electrochemistry, biological population models, and electromagnetics. Scientific and technical phenomena have been represented using fractional order differential operators to improve understanding of these phenomena. Moreover, as mentioned in reference [10], noninteger order systems have been utilized to accurately examine damping effects. The authors utilized fractional derivatives [11-14] to study chaotic systems. They also conducted studies on epidemic models [15-20] using fractional order derivatives. These derivatives are valuable for making predictions about past events and implementing necessary interventions in epidemics. Various authors have employed the fractional derivative to investigate the delay [21-22]. In a similar manner, they compose written content. The authors in reference [23] employed fractional derivatives to analyze systems of stochastic differential equations. These operators, known as fractional-order operators, have demonstrated consistent behavior over the last few decades, enabling the solution of complex problems in various scientific fields. Findings derived from fractional order calculations are more precise compared to those obtained from whole numbers. By consulting references [24-28], one can acquire comprehensive information regarding fractional calculations.

Non-integer differential equation structures offer the benefit of increased degrees of freedom and the inclusion of the memory effect in the model. We employ fractional conformable order differential equations [29-30] in conjunction with a mathematical model for Covid-19. CD does not contain any memory terms and is occasionally seen as a fractional order local differential operator. A number of academics have lately employed this operator in their research; for further details, refer to [31-32]. The conformable fractional operator [31-32] addresses the limitations of prior fractional operators and provides the following benefits: it enables standard calculus operations such as Rolle's theorem, the product of two functions, the derivative of the quotient of two functions, and the mean value theorem.

Furthermore, mathematical models including fractional derivatives are built upon memory systems that are present in several biological systems. The references [33-38] encompass the latest research conducted in this particular area.

The conformable derivative (CD) is a fractional local differential operator that does not include a memory term. A recent project has been finished. Based on the above logic, employing fractional differential operators to examine diverse real-world issues is more accurate than utilizing regular derivatives. Due to their reduced flexibility and non-local nature compared to integer derivatives, fractional order derivatives offer a higher degree of freedom in approximating real data than classical derivatives. Given the presence of these characteristics, we employed the fractional derivative formulation of the Covid 19 model. In this

context, the current study extends the Covid-19 model (1) from integer to fractional order. We analyze the model in the context of CD. Model (2) encapsulates our cognitive framework.

Equation (1) can be rewritten as follows:

$$\begin{aligned} T_{\zeta_0}^q S(t) &= \Lambda - \phi_c I(t) S(t) - \mu S(t) + v_3 R(t), \\ T_{\zeta_0}^q E(t) &= \phi_c I(t) S(t) - (\sigma + \mu) E(t), \\ T_{\zeta_0}^q I(t) &= \sigma E(t) - (\alpha + v_2 + \delta + \mu) I(t) + v_1 R(t), \quad (2) \\ T_{\zeta_0}^q Q(t) &= \alpha I(t) - (\theta + \mu) Q(t), \\ T_{\zeta_0}^q R(t) &= \theta Q(t) - (v_1 + v_3 + \mu) R(t) + v_2 I(t), \end{aligned}$$

In addition, the initial conditions are described as

$$S(0)=S_0, E(0)=E_0, I(0)=I_0, Q(0)=Q_0, R(0)=R_0 \text{ and } \begin{cases} S(0)=S_0 \geq 0 \\ E(0)=E_0 \geq 0 \\ I(0)=I_0 \geq 0 \\ Q(0)=Q_0 \geq 0 \\ R(0)=R_0 \geq 0 \end{cases} \quad (3)$$

Fractional differential problems exhibit a greater level of flexibility, as previously mentioned. However, obtaining an accurate analytical solution for each problem is a highly laborious endeavor. Furthermore, calculating the analytical and closed solutions to the aforementioned challenges can frequently be a challenge. Therefore, there is a continuing demand for the most effective numerical approximation techniques. In order to analyze the area stated above for simulations, scientists have developed a range of computational tools. Due to our ability to understand the resolution of these difficulties and investigate their potential applications Several numerical approaches for fractional order difficulties have already been developed and are commonly referred to as [38-40]. The qualitative theory is a powerful tool for determining the existence of a solution to the problem with fractional order. Furthermore, the presence and singularity of the solution are vital stages in the procedure. In order to obtain the desired findings, we commonly utilize fixed point theory and functional analytic methods [41-44].

In addition, we employ a numerical method outlined in reference [45] to approximately solve the given model (4) in order to replicate our findings. We will employ Euler's methodology, which is the most straightforward technique in the literature, to estimate the solution. Furthermore, the method proposed in [46-47] has been used to prove the positivity and boundedness of the solution. Recently, researchers have devised efficient techniques for solving nonlinear fractional integral equations and nonlinear Volterra-Fredholm integral equations [48-50]. Studies on random differential have been undertaken in recent years [51-53].

The study is designed as follows: Chapter 2 contains basic definitions. Chapter 3 contains the theoretical

analysis of the Covid 19 model. Chapter 4 contains the solutions obtained from the conformable fractional differential transformation method (CFDTM) and variational iteration method (VIM) and the comparison of these solutions. The fifth section contains the conclusion.

PRELIMINARIES

Definition 1. The conformable derivative of function $\aleph: [\zeta_0, \infty) \rightarrow \mathbb{R}$ with order $p \in (0,1]$ is given [31-32,39-40]

$$T_{\zeta_0}^p \aleph(\zeta) = \lim_{h \rightarrow \zeta_0} \frac{\aleph(\zeta + h\zeta^{1-p}) - \aleph(\zeta)}{h}, \text{ for every } \zeta > \zeta_0, \text{ on condition that if } T_{\zeta_0}^p \chi(\zeta) = \lim_{\zeta \rightarrow \zeta_0} D_p^{\zeta_0} \aleph(\zeta).$$

Definition 2. The conformable fractional integral of a function function $\aleph: [\zeta_0, \infty) \rightarrow \mathbb{R}$ with order $p \in (0,1]$ is given by

$$I_{\zeta_0}^{\zeta} \aleph(\zeta) = \int_{\zeta_0}^{\zeta} (\Phi - \zeta_0)^p \aleph(\Phi) d\Phi, \text{ for every } \zeta > \zeta_0, \text{ on condition that the integral on the right exists.}$$

Lemma 1. Under the continuity of $\aleph: [\zeta_0, \infty) \rightarrow \mathbb{R}$, we have the given results.

$$T_{\zeta_0}^p [I_{\zeta_0}^{\zeta} \aleph(\zeta)] = \aleph(\zeta). \quad p \in (0,1], \text{ for every } \zeta > \zeta_0.$$

Lemma 2. Besides, we have the following result.

$$I_{\zeta_0}^{\zeta} [T_{\zeta_0}^p \aleph(\zeta)] = \aleph(\zeta) - \aleph(\zeta_0), p \in (0,1].$$

THEORETICAL ANALYSIS OF THE COVID-19 MODEL

Positivity and Boundedness

We follow the procedure described in [46-47] and we can conclude that the solution of the considered model is positive:

$$\begin{cases} T_{\zeta_0}^p S(\zeta)|_{S=0} = \Lambda + v_3 R > 0 & (4a) \\ T_{\zeta_0}^p E(\zeta)|_{E=0} = \phi_c I S > 0 & (4b) \\ T_{\zeta_0}^p I(\zeta)|_{I=0} = \sigma E + v_1 R > 0 & (4c) \\ T_{\zeta_0}^p Q(\zeta)|_{Q=0} = \alpha I > 0 & (4d) \\ T_{\zeta_0}^p R(\zeta)|_{R=0} = \theta Q + v_2 I > 0. & (4e) \end{cases}$$

Thus, the Covid-19 model is positive if the initial conditions are positive.

Theorem 3.1.1. The Covid-19 model is bounded and the existence holds in the feasible region given by

$$\Omega = \left\{ (S, E, I, Q, R) \in R_+^5 : S + E + I + Q + R \leq \frac{\Lambda}{\mu} \right\}. \quad (5)$$

Proof: Let N be total population at time say ζ . Thus, we have

$$N(\zeta) = S(\zeta) + E(\zeta) + I(\zeta) + Q(\zeta) + R(\zeta). \quad (6)$$

Taking CFOD $p > 0$ of (6), one has

$$\begin{aligned} T_{\zeta_0}^p[N(\zeta)] &= T_{\zeta_0}^p[S(\zeta)] + T_{\zeta_0}^p[E(\zeta)] + T_{\zeta_0}^p[I(\zeta)] \\ &\quad + T_{\zeta_0}^p[Q(\zeta)] + T_{\zeta_0}^p[R(\zeta)] \\ &= \Lambda - \mu N(\zeta) - \delta I(\zeta) \leq \Lambda - \mu N(\zeta). \end{aligned} \quad (7)$$

Since $0 < I(\zeta) \leq N(\zeta)$ the term $\delta I(\zeta)$ is neglected. As a result, the solution is limited, and we can express the appropriate region as shown in (5). Taking conformable Laplace transform of both sides, and using $\zeta \rightarrow \infty$, we have $N(\zeta) \leq \frac{\Lambda}{\mu}$.

Equilibrium Points

The disease epidemic and free equilibrium points have been computed in [9] as $E_0 = (\frac{\Lambda}{\mu}, 0, 0, 0, 0)$ and $E^* = (S^*, E^*, I^*, Q^*, R^*)$ where

$$\begin{aligned} S^* &= \frac{a_2(a_1a_3a_4 - a\theta v_1 - a_3v_1v_2)}{\phi_c\sigma a_3a_4} \\ E^* &= \frac{(\Lambda\phi_c\sigma a_3a_4 + a\mu\theta a_2v_1 - \mu a_1a_2a_3a_4 + \mu a_2a_3v_1v_2)(a\theta v_1 - a_1a_3a_4 + a_3v_1v_2)}{(a\sigma\theta v_3 + a\theta a_2v_1 + \sigma a_3v_2v_3 - a_1a_2a_3a_4 + a_2a_3v_1v_2)\phi_c\sigma a_3a_4} \\ I^* &= \frac{\mu a_1a_2a_3a_4 - \Lambda\phi_c\sigma a_3a_4 - a\mu\theta a_2v_1 - \mu a_2a_3v_1v_2}{\phi_c(a\sigma\theta v_3 + a\theta a_2v_1 + \sigma a_3v_2v_3 - a_1a_2a_3a_4 + a_2a_3v_1v_2)} \\ Q^* &= \frac{a(\mu a_1a_2a_3a_4 - \Lambda\phi_c\sigma a_3a_4 - a\mu\theta a_2v_1 - \mu a_2a_3v_1v_2)}{\phi_c(a\sigma\theta v_3 + a\theta a_2v_1 + \sigma a_3v_2v_3 - a_1a_2a_3a_4 + a_2a_3v_1v_2)a_3} \\ R^* &= \frac{(\mu a_1a_2a_3a_4 - \Lambda\phi_c\sigma a_3a_4 - a\mu\theta a_2v_1 - \mu a_2a_3v_1v_2)}{(a\sigma\theta v_3 + a\theta a_2v_1 + \sigma a_3v_2v_3 - a_1a_2a_3a_4 + a_2a_3v_1v_2)} \times \frac{(a\theta + a_3v_2)}{\phi_c a_3a_4} \end{aligned}$$

We get the equations. Here, $a_1 = (\alpha + v_2 + \delta + \mu)$, $a_2 = (\sigma + \mu)$, $a_3 = (\theta + \mu)$ and $a_4 = (v_1 + v_3 + \mu)$

The Basic Reproduction Number (\mathfrak{R}_0)

\mathfrak{R}_0 denotes the mean number of secondary cases that arise from a patient, who is infected by that patient, in a community where everyone is vulnerable to the infectious disease. The term “ \mathfrak{R}_0 ” denotes the fundamental reproduction number of the Covid-19 model. It is employed in [9] for the purpose of determining the next generation matrix

technique. The following equation provides the numerical value.

$$\mathfrak{R}_0 = \frac{\phi_c \Lambda \sigma}{\mu(\sigma + \mu)(\alpha + v_2 + \delta + \mu)}$$

Based on the value of \mathfrak{R}_0 , there are three potential outcomes for the transmission or decline of a disease, which are as follows:

If the value of \mathfrak{R}_0 is less than or equal to 1, each existing infection results in less than one new infection. In this scenario, the sickness undergoes a gradual decrease and ultimately comes to an end. If the basic reproduction number \mathfrak{R}_0 is equal to 1, each existing function results in a new infection. The sickness remains extant, although it does not propagate. If the basic reproduction number \mathfrak{R}_0 is greater than 1, each existing infection leads to the occurrence of numerous new infections. The pathogen is transmitted to humans, leading to an outbreak of the disease. Figure 1 displays the three-dimensional profile of \mathfrak{R}_0 . We utilize the quantitative values presented in Table 2.

Analyzed was the impact of parameter modifications on the Basic Reproduction Number, utilizing the forward normalized sensitivity index. Contour plotting is a valuable and efficient graphical method frequently employed to present results of the Basic Reproduction Number. These

Table 1. Description of variables and parameters of the model (1)

Variable	Description
$S(t)$	At time t, the number of susceptible humans was
$E(t)$	Number of people who were exposed at time t
$I(t)$	At time t, the number of infectious humans was
$Q(t)$	Humans in quarantine at time t
$R(t)$	At time t, the number of recovered humans was

Table 2. Parameter values used in the model [18-19] [obtained from authors solution]

Parameter	Definition	Value
Λ	Recovery rate of individuals	750
ϕ_c	Contact rate for Covid-19 transmission	0.0000124
σ	Exposure rate of individuals	0.000011618
μ	Rate of natural deaths	0.00324588
v_2	Relapse rate of individuals	0.001466848
δ	Death rate from Covid-19	0.00286
θ	Survival rate of individuals in quarantine	0.0766169
α	Detection rate of infectious individuals	0.010939586
v_1	Survival rate of infectious people	0.1109289
v_3	Rate of returning individuals to the susceptible class	0.0022927

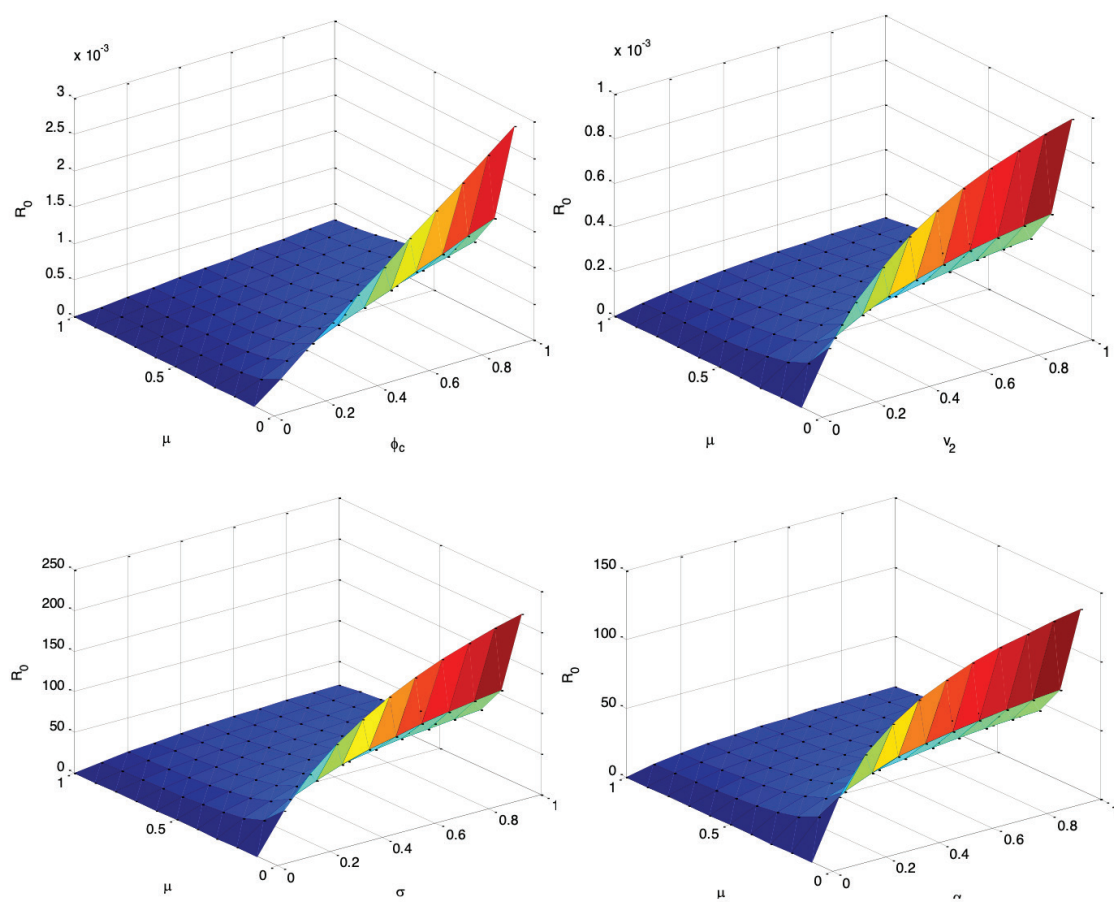


Figure 1. Three-dimensional representation of the \mathfrak{R}_0 value in the Covid-19 model

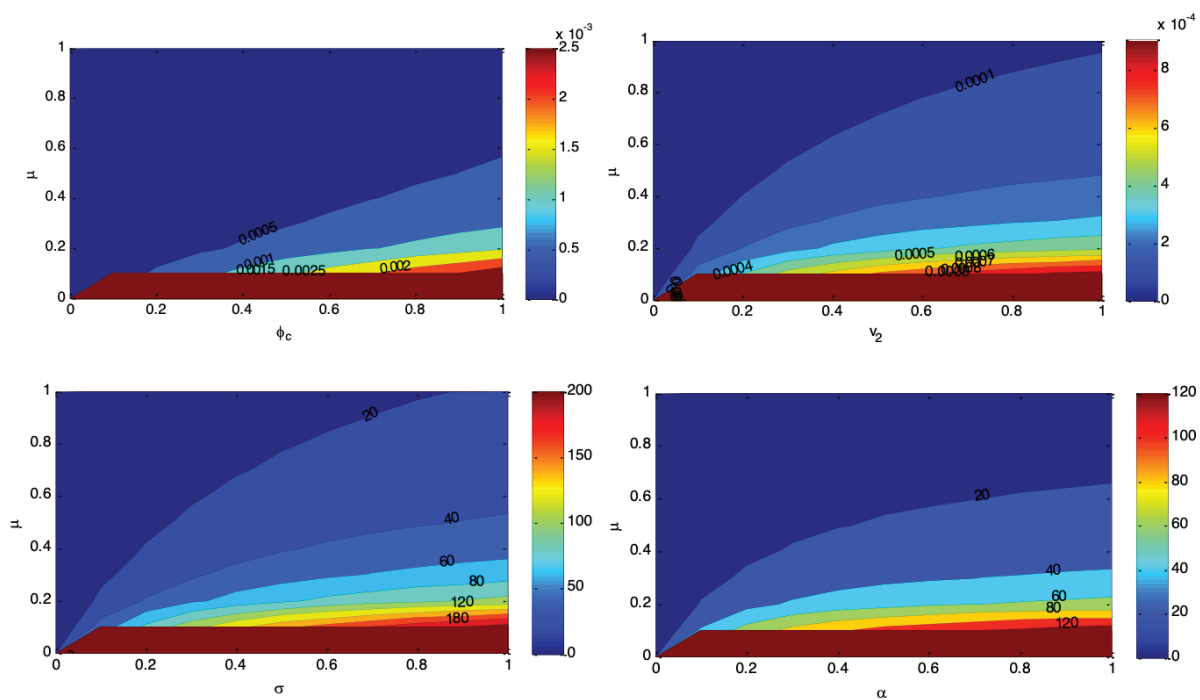


Figure 2. Contour plot of representation for \mathfrak{R}_0 of the Covid-19 model.

plots are especially valuable for identifying and analyzing the spread of shocks and abrupt changes.

NUMERICAL SCHEME FOR THE COVID-19 MODEL

The Conformable Fractional Differential Transformation Method

Assume that \mathcal{F} is an infinitely differentiable function in $[20, 22]$ for some q with $0 < q \leq 1$. The fractional power series expansion of $\mathcal{F}(w)$ around the point $w = 0$ is as follows:

$$\mathcal{F}(w) = \sum_{k=0}^{\infty} \frac{w^{qk}}{q^{k!}} \left[(T_q \mathcal{F})^{(k)} \right]_{w=0}, \quad 0 < w < \mathcal{R}^{1/q}, \mathcal{R} > 0. \quad (8)$$

where, $\left[(T_q \mathcal{F})^{(k)} \right]_{w=0}$ denotes the application of the fractional derivative for k times. Conformable fractional differential transform of $\mathcal{F}(w)$ is defined as

$$\mathcal{H}_q(k) = \frac{1}{q^{k!}} \left[(T_q \mathcal{F})^{(k)} \right]_{w=0} \quad (9)$$

The definition of the inverse conformable fractional differential transform of $\mathcal{H}(k)$ is as follows:

$$\mathcal{F}(w) = \sum_{k=0}^{\infty} w^{qk} \mathcal{H}_q(k) = \sum_{k=0}^{\infty} \frac{w^{qk}}{q^{k!}} \left[(T_q \mathcal{F})^{(k)} \right]_{w=0} \quad (10)$$

The conformable differential transform approach involves performing fundamental mathematical operations.

(i) If $\mathcal{F}(w) = (w - w_0)^p$, then $\mathcal{H}_q(k) = \delta(k - (p/\alpha))$, where

$$\delta(k) = \begin{cases} 1, & k = 0 \\ 0, & k \neq 0 \end{cases} \quad (11)$$

(ii) If $\mathcal{F}(w) = T_q u(w)$, then $\mathcal{H}_q(k) = q(k+1)U_q(k+1)$.

Application of conformable fractional differential transform Method for Covid-19 model

$$\begin{aligned} q(k+1)S_q(k+1) &= \Lambda S(k) - \phi_c \sum_{r=0}^k I_q(r)S_q(k-r) - \mu S_q(k) + v_3 R_q(k) \\ q(k+1)E_q(k+1) &= \phi_c \sum_{r=0}^k I_q(r)S_q(k-r) - (\sigma + \mu)E_q(k) \\ q(k+1)I_q(k+1) &= \sigma E_q(k) - (\alpha + v_2 + \delta + \mu)I_q(k) + v_1 R_q(k) \\ q(k+1)Q_q(k+1) &= \alpha I_q(k) - (\theta + \mu)Q_q(k) \\ q(k+1)R_q(k+1) &= \theta Q_q(k) - (v_1 + v_3 + \mu)R_q(k) + v_2 I_q(k) \end{aligned} \quad (12)$$

Hence, recurrence relation is obtained as

$$\begin{aligned} S_q(k+1) &= \frac{1}{q(k+1)} \left[\Lambda S(k) - \phi_c \sum_{r=0}^k I_q(r)S_q(k-r) - \mu S_q(k) + v_3 R_q(k) \right] \\ E_q(k+1) &= \frac{1}{q(k+1)} \left[\phi_c \sum_{r=0}^k I_q(r)S_q(k-r) - (\sigma + \mu)E_q(k) \right] \\ I_q(k+1) &= \frac{1}{q(k+1)} \left[\sigma E_q(k) - (\alpha + v_2 + \delta + \mu)I_q(k) + v_1 R_q(k) \right] \\ Q_q(k+1) &= \frac{1}{q(k+1)} \left[\alpha I_q(k) - (\theta + \mu)Q_q(k) \right] \\ R_q(k+1) &= \frac{1}{q(k+1)} \left[\theta Q_q(k) - (v_1 + v_3 + \mu)R_q(k) + v_2 I_q(k) \right] \end{aligned} \quad (13)$$

With initial conditions, $S(0) = 5000$, $E(0) = 2003$, $I(0) = 416$, $Q(0) = 404$, $R(0) = 115$ and parameter values are given in table 2.

Variational Iteration Method

To illustrate the fundamental concept of the variational iteration method, let us examine the given nonlinear differential equation in operator form:

$$H(u(t)) + N(u(t)) = h(t). \quad (14)$$

H represents the linear operator, N represents the nonlinear operator, and h represents any real function referred to as the inhomogeneous term. The correction function corresponding to equation (14) is presented as follows:

$$u_{n+1}(t) = u_n(t) + \int_0^t \lambda \{ H u_n(s) + N \tilde{u}_n(s) - h(s) \} ds, \quad (15)$$

Here, λ is the general Lagrange multiplier [54-57], which is best described by variational theory [44], and $N \tilde{u}_n$ is constrained variation, i.e. $\delta N \tilde{u}_n = 0$.

Theorem 1. Consider a Banach space B equipped with a norm $\|\cdot\|$. Let the series $\sum_{i=0}^{\infty} u_i$ be defined in B . Assume that the initial guess $y_0 = u_0$ is contained within the solution ball $\gamma(x)$. The series solution $\sum_{i=0}^{\infty} u_i$ converges if there is a value of r for which the inequality [54] $\|u_{n+1}\| \leq r \|u_n\|$ holds.

Theorem 2. Examine the second conformable differential equation. The variational iteration formula is expressed as follows:

$$\begin{aligned} S_{n+1}(t) &= S_n(t) - I_q \{ T_q S_n(t) - \Lambda + \phi_c I_n(t) S_n(t) + \mu S_n(t) - v_3 R_n(t) \}, \\ E_{n+1}(t) &= E_n(t) - I_q \{ T_q E_n(t) - \phi_c I_n(t) S_n(t) + (\sigma + \mu) E_n(t) \}, \\ I_{n+1}(t) &= I_n(t) - I_q \{ T_q I_n(t) - \sigma E_n(t) + (\alpha + v_2 + \delta + \mu) I_n(t) - v_1 R_n(t) \}, \\ Q_{n+1}(t) &= Q_n(t) - I_q \{ T_q Q_n(t) - \alpha I_n(t) + (\theta + \mu) Q_n(t) \}, \\ R_{n+1}(t) &= R_n(t) - I_q \{ T_q R_n(t) - \theta Q_n(t) + (v_1 + v_3 + \mu) R_n(t) - v_2 I_n(t) \}, \end{aligned} \quad (16)$$

where S_n , E_n , I_n , Q_n , R_n are n th approximation, T_q is the conformable derivative of order q , and I_q is the fractional integral of order $q \in (0, 1]$

Proof. Equation (2) may be rewritten equivalently as

$$\begin{aligned}
T_q S(t) - \Lambda + \phi_c I(t) S(t) + \mu S(t) - v_3 R(t) &= 0, \\
T_q E(t) - \phi_c I(t) S(t) + (\sigma + \mu) E(t) &= 0, \\
T_q I(t) - \sigma E(t) + (\alpha + v_2 + \delta + \mu) I(t) - v_1 R(t) &= 0, \\
T_q Q(t) - \alpha I(t) + (\theta + \mu) Q(t) &= 0, \\
T_q R(t) - \theta Q(t) + (v_1 + v_3 + \mu) R(t) - v_2 I(t) &= 0,
\end{aligned} \quad (17)$$

Multiplying equation (17) by a general Lagrange multiplier $\lambda_1(t)$, $\lambda_2(t)$, $\lambda_3(t)$, $\lambda_4(t)$ and $\lambda_5(t)$ yields

$$\begin{aligned}
\lambda_1(t) \{T_q S(t) - \Lambda + \phi_c I(t) S(t) + \mu S(t) - v_3 R(t)\} &= 0, \\
\lambda_2(t) \{T_q E(t) - \phi_c I(t) S(t) + (\sigma + \mu) E(t)\} &= 0, \\
\lambda_3(t) \{T_q I(t) - \sigma E(t) + (\alpha + v_2 + \delta + \mu) I(t) - v_1 R(t)\} &= 0, \\
\lambda_4(t) \{T_q Q(t) - \alpha I(t) + (\theta + \mu) Q(t)\} &= 0, \\
\lambda_5(t) \{T_q R(t) - \theta Q(t) + (v_1 + v_3 + \mu) R(t) - v_2 I(t)\} &= 0,
\end{aligned} \quad (18)$$

Now, upon applying I_q to the both sides of equation (18) will give

$$\begin{aligned}
I_q [\lambda_1(t) \{T_q S(t) - \Lambda + \phi_c I(t) S(t) + \mu S(t) - v_3 R(t)\}] &= 0, \\
I_q [\lambda_2(t) \{T_q E(t) - \phi_c I(t) S(t) + (\sigma + \mu) E(t)\}] &= 0, \\
I_q [\lambda_3(t) \{T_q I(t) - \sigma E(t) + (\alpha + v_2 + \delta + \mu) I(t) - v_1 R(t)\}] &= 0, \\
I_q [\lambda_4(t) \{T_q Q(t) - \alpha I(t) + (\theta + \mu) Q(t)\}] &= 0, \\
I_q [\lambda_5(t) \{T_q R(t) - \theta Q(t) + (v_1 + v_3 + \mu) R(t) - v_2 I(t)\}] &= 0,
\end{aligned} \quad (19)$$

Then, the correction functional of equation (2) will be read as follows:

$$\begin{aligned}
S_{n+1}(t) &= S_n(t) + I_q [\lambda_1(t) \{T_q S_n(t) - \Lambda + \phi_c \bar{S}_n(t) \bar{I}_n(t) + \mu \bar{S}_n(t) - v_3 \bar{R}_n(t)\}], \\
E_{n+1}(t) &= E_n(t) + I_q [\lambda_2(t) \{T_q E_n(t) - \phi_c \bar{I}_n(t) \bar{S}_n(t) + (\sigma + \mu) \bar{E}_n(t)\}], \\
I_{n+1}(t) &= I_n(t) + I_q [\lambda_3(t) \{T_q I_n(t) - \sigma \bar{E}_n(t) + (\alpha + v_2 + \delta + \mu) \bar{I}_n(t) - v_1 \bar{R}_n(t)\}], \\
Q_{n+1}(t) &= Q_n(t) + I_q [\lambda_4(t) \{T_q Q_n(t) - \alpha \bar{I}_n(t) + (\theta + \mu) \bar{Q}_n(t)\}], \\
R_{n+1}(t) &= R_n(t) + I_q [\lambda_5(t) \{T_q R_n(t) - \theta \bar{Q}_n(t) + (v_1 + v_3 + \mu) \bar{R}_n(t) - v_2 \bar{I}_n(t)\}],
\end{aligned} \quad (20)$$

In this case, calculating the value of $\lambda_i(t)$, for $i = \{1, 2, 3, 4, 5\}$ from equation (20), which is a fractional integral functional, is difficult. Equation (20) can be written as:

$$\begin{aligned}
S_{n+1}(t) &= S_n(t) + \int_0^t \tau^{q-1} \left[\lambda_1(\tau) \left\{ \tau^{1-q} \frac{d}{d\tau} S_n(\tau) - \Lambda + \phi_c \bar{S}_n(\tau) \bar{I}_n(\tau) + \mu \bar{S}_n(\tau) - v_3 \bar{R}_n(\tau) \right\} \right] d\tau \\
E_{n+1}(t) &= E_n(t) + \int_0^t \tau^{q-1} \left[\lambda_2(\tau) \left\{ \tau^{1-q} \frac{d}{d\tau} E_n(\tau) - \phi_c \bar{I}_n(\tau) \bar{S}_n(\tau) + (\sigma + \mu) \bar{E}_n(\tau) \right\} \right] d\tau \\
I_{n+1}(t) &= I_n(t) + \int_0^t \tau^{q-1} \left[\lambda_3(\tau) \left\{ \tau^{1-q} \frac{d}{d\tau} I_n(\tau) - \sigma \bar{E}_n(\tau) + (\alpha + v_2 + \delta + \mu) \bar{I}_n(\tau) - v_1 \bar{R}_n(\tau) \right\} \right] d\tau \\
Q_{n+1}(t) &= Q_n(t) + \int_0^t \tau^{q-1} \left[\lambda_4(\tau) \left\{ \tau^{1-q} \frac{d}{d\tau} Q_n(\tau) - \alpha \bar{I}_n(\tau) + (\theta + \mu) \bar{Q}_n(\tau) \right\} \right] d\tau \\
R_{n+1}(t) &= R_n(t) + \int_0^t \tau^{q-1} \left[\lambda_5(\tau) \left\{ \tau^{1-q} \frac{d}{d\tau} R_n(\tau) - \theta \bar{Q}_n(\tau) + (v_1 + v_3 + \mu) \bar{R}_n(\tau) - v_2 \bar{I}_n(\tau) \right\} \right] d\tau
\end{aligned} \quad (21)$$

Where \bar{S}_n , \bar{E}_n , \bar{I}_n , \bar{Q}_n , and \bar{R}_n are the restricted variations with $\delta \bar{S}_n = 0$, $\delta \bar{E}_n = 0$, $\delta \bar{I}_n = 0$, $\delta \bar{Q}_n = 0$ and $\delta \bar{R}_n = 0$. From equation (21), we obtain

$$\begin{aligned}
\delta S_{n+1}(t) &= \delta S_n(t) + \delta \int_0^t \left[\lambda_1(\tau) \left\{ \frac{d}{d\tau} S_n(\tau) - \Lambda \tau^{q-1} \right. \right. \\
&\quad \left. \left. + \phi_c \tau^{q-1} \bar{S}_n(\tau) \bar{I}_n(\tau) + \mu \tau^{q-1} \bar{S}_n(\tau) - v_3 \tau^{q-1} \bar{R}_n(\tau) \right\} \right] d\tau
\end{aligned} \quad (22)$$

$$\begin{aligned}
\delta E_{n+1}(t) &= \delta E_n(t) + \delta \int_0^t \left[\lambda_2(\tau) \left\{ \frac{d}{d\tau} E_n(\tau) - \phi_c \tau^{q-1} \bar{I}_n(\tau) \bar{S}_n(\tau) \right. \right. \\
&\quad \left. \left. + (\sigma + \mu) \tau^{q-1} \bar{E}_n(\tau) \right\} \right] d\tau
\end{aligned} \quad (23)$$

$$\begin{aligned}
\delta I_{n+1}(t) &= \delta I_n(t) + \delta \int_0^t \left[\lambda_3(\tau) \left\{ \frac{d}{d\tau} I_n(\tau) - \sigma \tau^{q-1} \bar{E}_n(\tau) \right. \right. \\
&\quad \left. \left. + (\alpha + v_2 + \delta + \mu) \tau^{q-1} \bar{I}_n(\tau) - v_1 \tau^{q-1} \bar{R}_n(\tau) \right\} \right] d\tau
\end{aligned} \quad (24)$$

$$\begin{aligned}
\delta Q_{n+1}(t) &= \delta Q_n(t) + \delta \int_0^t \left[\lambda_4(\tau) \left\{ \frac{d}{d\tau} Q_n(\tau) - \alpha \tau^{q-1} \bar{I}_n(\tau) \right. \right. \\
&\quad \left. \left. + (\theta + \mu) \tau^{q-1} \bar{Q}_n(\tau) \right\} \right] d\tau
\end{aligned} \quad (25)$$

$$\begin{aligned}
\delta R_{n+1}(t) &= \delta R_n(t) + \delta \int_0^t \left[\lambda_5(\tau) \left\{ \frac{d}{d\tau} R_n(\tau) - \theta \tau^{q-1} \bar{Q}_n(\tau) \right. \right. \\
&\quad \left. \left. + (v_1 + v_3 + \mu) \tau^{q-1} \bar{R}_n(\tau) - v_2 \tau^{q-1} \bar{I}_n(\tau) \right\} \right] d\tau
\end{aligned} \quad (26)$$

Using integration by parts, equation (22) becomes for equations (23), (24), (25) and (26) are similar to proof of equation (22)

$$\begin{aligned}
\delta S_{n+1}(t) &= \delta S_n(t) + \delta \left(\lambda_1(t) S_n(t) - \int_0^t \lambda_1'(\tau) S_n(\tau) d\tau \right) \\
&= \left(1 + \lambda_1(t) \delta S_n(t) - \delta \int_0^t \lambda_1'(\tau) S_n(\tau) d\tau \right) \\
\delta E_{n+1}(t) &= \left(1 + \lambda_2(t) \delta E_n(t) - \delta \int_0^t \lambda_2'(\tau) E_n(\tau) d\tau \right) \\
\delta I_{n+1}(t) &= \left(1 + \lambda_3(t) \delta I_n(t) - \delta \int_0^t \lambda_3'(\tau) I_n(\tau) d\tau \right) \\
\delta Q_{n+1}(t) &= \left(1 + \lambda_4(t) \delta Q_n(t) - \delta \int_0^t \lambda_4'(\tau) Q_n(\tau) d\tau \right) \\
\delta R_{n+1}(t) &= \left(1 + \lambda_5(t) \delta R_n(t) - \delta \int_0^t \lambda_5'(\tau) R_n(\tau) d\tau \right)
\end{aligned} \quad (27)$$

The lagrange multipliers $\lambda_1(t)$, $\lambda_2(t)$, $\lambda_3(t)$, $\lambda_4(t)$ and $\lambda_5(t)$ can be obtained by $\lambda_i'(t) = 0$ for all $i = \{1, 2, 3, 4, 5\}$ with boundary condition: $1 + \lambda_i(t) = 0$ for all $i = \{1, 2, 3, 4, 5\}$. Solving the last initial value problem for λ_i for all $i = \{1, 2, 3, 4, 5\}$, the general Lagrange multiplier λ_i is found to be

$$\lambda_i = -1, \text{ for all } i = \{1, 2, 3, 4, 5\} \quad (28)$$

Thus, substituting λ_i into the corresponding smoothing function (20) yields the iteration formula:

$$\begin{aligned}
S_{n+1}(t) &= S_n(t) - I_q \{ T_q S_n(t) - \Lambda + \phi_c \tilde{S}_n(t) \tilde{I}_n(t) + \mu \tilde{S}_n(t) - v_3 \tilde{R}_n(t) \} \\
E_{n+1}(t) &= E_n(t) - I_q \{ T_q E_n(t) - \phi_c \tilde{I}_n(t) \tilde{S}_n(t) + (\sigma + \mu) \tilde{E}_n(t) \} \\
I_{n+1}(t) &= I_n(t) - I_q \{ T_q I_n(t) - \sigma \tilde{E}_n(t) + (\alpha + v_2 + \delta + \mu) \tilde{I}_n(t) - v_1 \tilde{R}_n(t) \} \quad (29) \\
Q_{n+1}(t) &= Q_n(t) - I_q \{ T_q Q_n(t) - \alpha \tilde{I}_n(t) + (\theta + \mu) \tilde{Q}_n(t) \} \\
R_{n+1}(t) &= R_n(t) - I_q \{ T_q R_n(t) - \theta \tilde{Q}_n(t) + (v_1 + v_3 + \mu) \tilde{R}_n(t) - v_2 \tilde{I}_n(t) \}
\end{aligned}$$

Application of the variational iteration method

Applying the variational iteration method using Theorem 1,

$$\begin{aligned}
S_{n+1}(t) &= S_n(t) - \int_0^t \tau^{q-1} \left\{ \tau^{1-q} \frac{d}{d\tau} S_n(\tau) - \Lambda + \phi_c I_n(\tau) S_n(\tau) + \mu S_n(\tau) - v_3 R_n(\tau) \right\} d\tau \\
E_{n+1}(t) &= E_n(t) - \int_0^t \tau^{q-1} \left\{ \tau^{1-q} \frac{d}{d\tau} E_n(\tau) - \phi_c I_n(\tau) S_n(\tau) + (\sigma + \mu) E_n(\tau) \right\} d\tau \\
I_{n+1}(t) &= I_n(t) - \int_0^t \tau^{q-1} \left\{ \tau^{1-q} \frac{d}{d\tau} I_n(\tau) - \sigma E_n(\tau) + (\alpha + v_2 + \delta + \mu) I_n(\tau) - v_1 R_n(\tau) \right\} d\tau \quad (30) \\
Q_{n+1}(t) &= Q_n(t) - \int_0^t \tau^{q-1} \left\{ \tau^{1-q} \frac{d}{d\tau} Q_n(\tau) - \alpha I_n(\tau) + (\theta + \mu) Q_n(\tau) \right\} d\tau \\
R_{n+1}(t) &= R_n(t) - \int_0^t \tau^{q-1} \left\{ \tau^{1-q} \frac{d}{d\tau} R_n(\tau) - \theta Q_n(\tau) + (v_1 + v_3 + \mu) R_n(\tau) - v_2 I_n(\tau) \right\} d\tau
\end{aligned}$$

With initial conditions, $S(0) = 5000$, $E(0) = 2003$, $I(0) = 416$, $Q(0) = 404$, $R(0) = 115$ and parameter values are given in table 2, we obtain

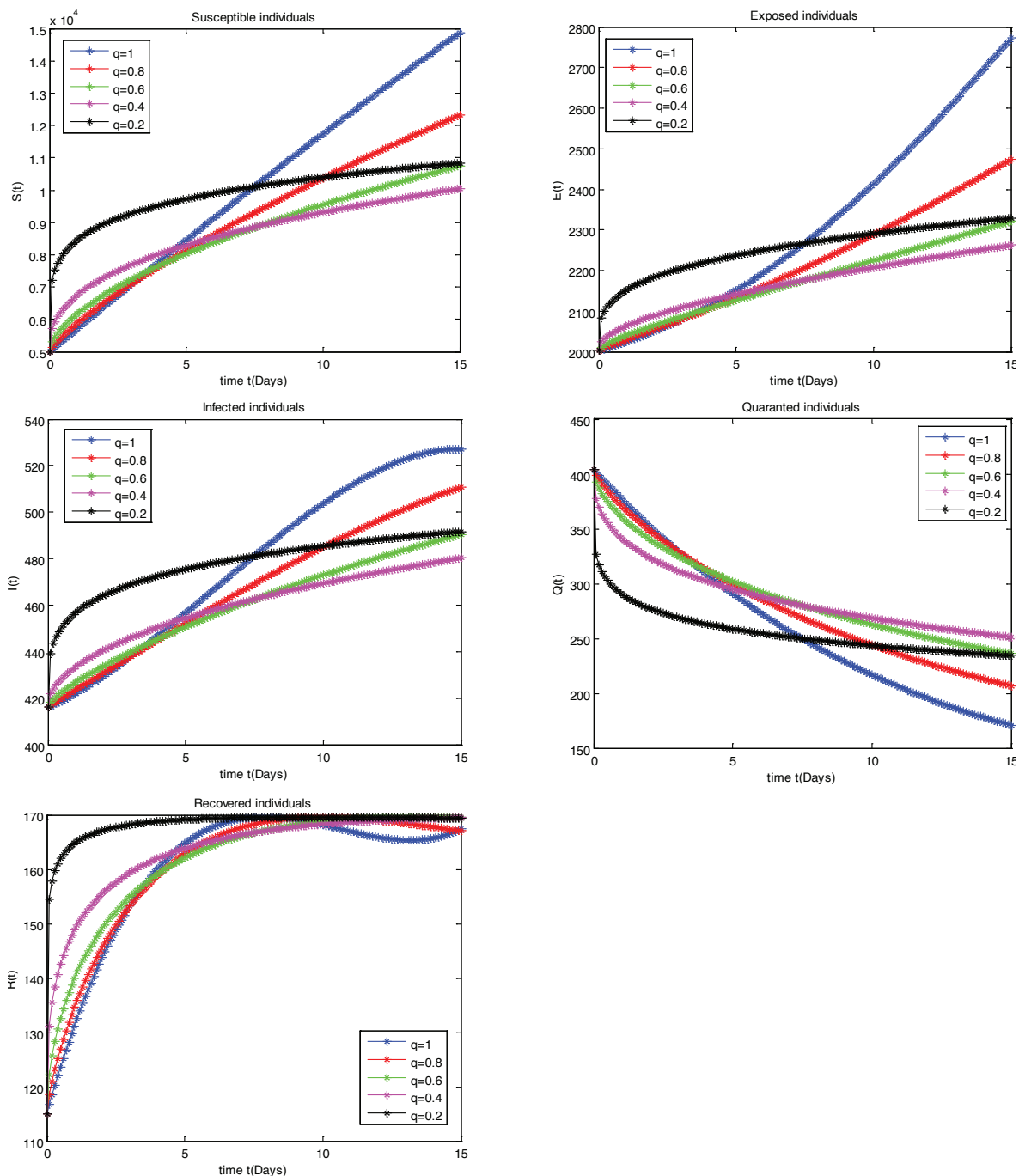


Figure 2. The CDTM solutions of for system (13) at different q values.

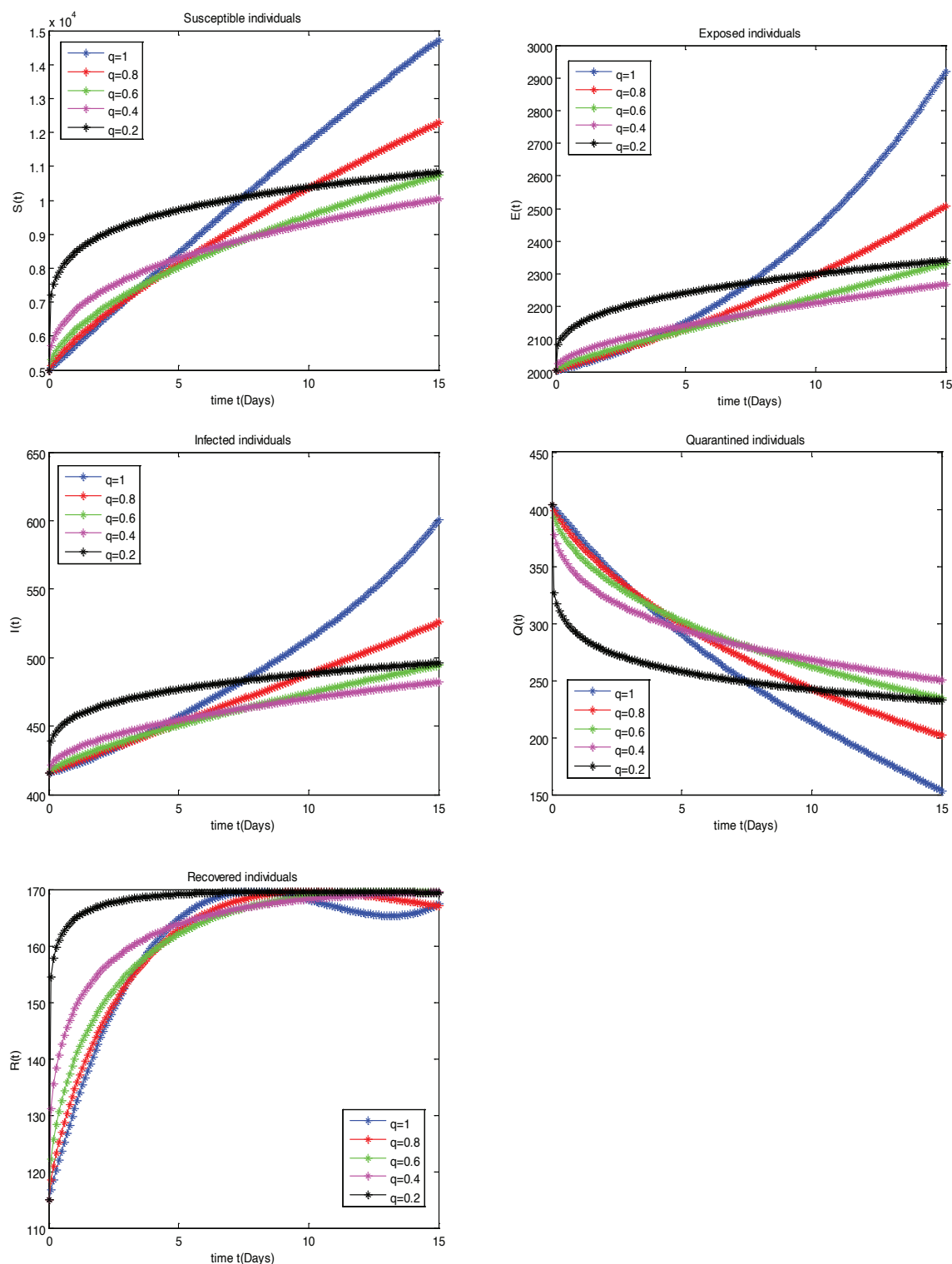


Figure 3. The VIM solutions of for system (30) at different q values.

Figure 2 illustrates that the number of susceptible, exposed, and infected individuals grows as the fractional order derivative drops during the first seven days. However, after this period, the number of individuals in these

categories decreases. The number of individuals who have recovered increases over time, whereas the number of individuals under quarantine decreases as the fractional order derivative decreases.

Figure 3 displays the VIM solutions for system (30) at various q values.

The result of equation (4)'s epidemic system is completely in line with the result of the conformable fractional differential transformation approach. Figure 2-3. Figure 3 demonstrates that as the fractional order derivative declines, there is an increase in the number of susceptible, exposed, and infected individuals during the initial 7 days, followed by a reduction after 7 days. As the value of the fractional order derivative declines, there is an observed increase in the number of persons who have recovered over time, while the number of individuals in quarantine decreases. It is evident that the solution acquired from the CFDTM in Figure 2 and the solutions produced from the VIM method in Figure 3 are compatible for various values of the fractional order q [58].

Below, the approximate analytical $S(t)$ solution obtained from the VIM method and the convergence analysis for this solution are given.

$$\begin{aligned} S(t) = & 5000. + 708.2422605t - 0.02762284236t^3 \\ & - 3.112751154t^2 - .4759874044e - 6t^6 \\ & + .1590043949e - 3t^5 - .6340772020e - 3t^4 \\ & - .1437275197e - 20t^{11} + .3080875470e - 14t^{10} \\ & + .8428734232e - 12t^9 - .2762956380e - 9t^8 \\ & - .7677240689e - 9t^7 \end{aligned}$$

If we examine the convergence by choosing $t = 1, q = 1$.

$$\begin{aligned} r_1: \frac{\|S_2\|}{\|S_1\|} &= \frac{\|-3.112751154t^2\|}{\|708.2422605t\|} = 0.0044 < 1 \\ r_2: \frac{\|S_3\|}{\|S_2\|} &= \frac{\|-0.02762284236t^3\|}{\|-3.112751154t^2\|} = 0.0089 < 1 \\ r_3: \frac{\|S_4\|}{\|S_3\|} &= \frac{\|-.6340772020e - 3t^4\|}{\|-0.02762284236t^3\|} = 0.0230 < 1 \\ r_4: \frac{\|S_5\|}{\|S_4\|} &= \frac{\|+.1590043949e - 3t^5\|}{\|-.6340772020e - 3t^4\|} = 0.2508 < 1 \end{aligned}$$

⋮

It converges because its values are less than 1 [54-55].

Table 3. Table for numerical solutions of the Covid-19 model for $q = 0.9$ with CFDTM

t	$S(t)$	$E(t)$	$I(t)$	$Q(t)$	$R(t)$
0.0	5000.	2003.	416.	404.	115.
0.1	5096.186981	2005.678857	416.7191853	400.2668463	117.4063418
0.2	5181.260454	2008.163002	417.4071349	397.0205933	119.4249899
0.3	5262.087376	2010.629044	418.1047249	393.9860365	121.2472211
0.4	5340.155114	2013.111987	418.8165406	391.1008331	122.9215621
0.5	5416.169854	2015.627333	419.5424076	388.3340727	124.4747571
0.6	5490.546773	2018.183646	420.2805261	385.6667078	125.9251287
0.7	5563.559537	2020.786264	421.0283768	383.0855310	127.2867593
0.8	5635.402119	2023.438816	421.7830748	380.5806647	128.5712595
0.9	5706.219127	2026.143916	422.5415349	378.1443197	129.7886583
1.0	5776.122446	2028.903568	423.3005544	375.7701077	130.9479015

Table 4. Table for numerical solutions of the Covid-19 model for $q = 0.9$ with VIM

t	$S(t)$	$E(t)$	$I(t)$	$Q(t)$	$R(t)$
0.0	5000.	2003.	416.	404.	115.
0.1	5099.008371	2005.733396	416.7290149	400.1455378	117.5004699
0.2	5184.657369	2008.162796	417.3897214	396.8428549	119.6005287
0.3	5265.844571	2010.521633	418.0410085	393.7391713	121.5381523
0.4	5344.237772	2012.851421	418.6923496	390.7670265	123.3608975
0.5	5420.598995	2015.170437	419.3474747	387.8951332	125.0915734
0.6	5495.365463	2017.488820	420.0081702	385.1052755	126.7438936
0.7	5568.820372	2019.812931	420.6753546	382.3854843	128.3271556
0.8	5641.161773	2022.147076	421.3494972	379.7272671	129.8481617
0.9	5712.535743	2024.494343	422.0308120	377.1242679	131.3121552
1.0	5783.054353	2026.857034	422.7193594	374.5715396	132.7233368

Comparison

In order to compare accuracy of the obtained results by CFDTM and VIM, Table 3,4 are presented.

Once again, it has been noted that the solution derived from the Conformable Fractional Differential Transformation Method is consistent with the solution acquired from the variational iteration method.

CONCLUSION

In this study, we employed two numerical approaches to provide approximate solutions for the Covid 19 epidemic model. These techniques rely on conformable derivatives, which have recently become prominent. By employing the q -derivative, we initially redefined the concerted differential transformation method and variational iteration approach. Through the application of the suggested techniques to the Covid 19 epidemic model, we have showcased their effectiveness and precision. Our variational iteration method successfully obtained the approximate solution matching to the concerted differential transformation method, which is in total agreement with it. Moreover, our methods can be readily applied to a diverse array of epidemic models, such as fractional order avian influenza, swine flu, SIR, SEIR/SEIRS, and SIS, due to their simplicity in mathematical application to many physical problems.

AUTHORSHIP CONTRIBUTIONS

Authors equally contributed to this work.

DATA AVAILABILITY STATEMENT

The authors confirm that the data that supports the findings of this study are available within the article. Raw data that support the finding of this study are available from the corresponding author, upon reasonable request.

CONFLICT OF INTEREST

The author declared no potential conflicts of interest with respect to the research, authorship, and/or publication of this article.

AUTHORSHIP CONTRIBUTIONS

Authors equally contributed to this work.

ETHICS

There are no ethical issues with the publication of this manuscript.

REFERENCES

- [1] Abbey H. An examination of the Reed Frost theory of epidemics. *Hum Biol* 1952;24:201.
- [2] Kermack WO, McKendrick AG. A contribution to the mathematical theory of epidemics. *Proc R Soc Lond A Math Phys Sci* 1927;115:700–721. [\[CrossRef\]](#)
- [3] Hethcote HW. The mathematics of infectious diseases. *SIAM Rev* 2000;42:599–653. [\[CrossRef\]](#)
- [4] Anderson RM. The population dynamics of infectious diseases: theory and applications. New York: Springer; 2013.
- [5] Brauer F, Castillo-Chavez C. Mathematical models in population biology and epidemiology. 2nd ed. New York: Springer; 2012. p. 508. [\[CrossRef\]](#)
- [6] Murray JD. Mathematical biology: I. An introduction. 3rd ed. New York: Springer; 2007. Vol. 17.
- [7] Oliveira G. Refined compartmental models, asymptomatic carriers and COVID-19. *arXiv Preprint*. 2020. doi:10.1101/2020.04.14.20065128 [\[CrossRef\]](#)
- [8] Abou-Ismaïl A. Compartmental models of the COVID-19 pandemic for physicians and physician scientists. *SN Compr Clin Med*.2020;1. [\[CrossRef\]](#)
- [9] Abioye AI, Peter OJ, Ogunseye HA, Oguntolu FA, Oshinubi K, Ibrahim AA, Khan I. Mathematical model of COVID-19 in Nigeria with optimal control. *Results Phys* 2021;28:104598. [\[CrossRef\]](#)
- [10] Ray SS, Atangana A, Noutchie SC, Kurulay M, Bildik N, Kilicman A. Fractional calculus and its applications in applied mathematics and other sciences. *Math Probl Eng* 2014;849395. [\[CrossRef\]](#)
- [11] Li C, Peng G. Chaos in Chen's system with a fractional order. *Chaos Solit Fractals* 2004;22:443–450. [\[CrossRef\]](#)
- [12] Owolabi KM, Gómez-Aguilar JF, Fernández-Anaya G, Lavín-Delgado JE, Hernández-Castillo E. Modelling of chaotic processes with Caputo fractional order derivative. *Entropy* 2020;22:1027. [\[CrossRef\]](#)
- [13] Petráš I. A note on the fractional-order Chua's system. *Chaos Solit Fractals*. 2008;38:140–147. [\[CrossRef\]](#)
- [14] Atangana A, Koca I. Chaos in a simple nonlinear system with Atangana–Baleanu derivatives with fractional order. *Chaos Solit Fractals* 2016;447–454. [\[CrossRef\]](#)
- [15] Gozalez-Parra G, Arenas AJ, Chen-Charpentier BM. A fractional order epidemic model for the simulation of outbreaks of influenza A(H1N1). *Math Methods Appl Sci* 2014;37:2218–2226. [\[CrossRef\]](#)
- [16] Paul S, Mahata A, Mukherjee S, Roy B. Dynamics of SIQR epidemic model with fractional order derivative. *Partial Differ Equ Appl Math* 2022;5:100216. [\[CrossRef\]](#)
- [17] Area I, Batarfi H, Losada J, Nieto JJ, Shammakh W, Torres A. On a fractional order Ebola epidemic model. *Adv Differ Equ* 2015:278. [\[CrossRef\]](#)
- [18] Din A, Abidin MZ. Analysis of fractional-order vaccinated Hepatitis-B epidemic model with Mittag-Leffler kernels. *Math Model Numer Simul Appl* 2022;2:59–72. [\[CrossRef\]](#)
- [19] Ding Y, Wang Z, Ye H. Optimal control of a fractional-order HIV-immune system with memory. *IEEE Trans Control Syst Technol* 2011;99:1–7.

- [20] El-Shahed M, Alsaedi A. The fractional SIAC model and influenza A. *Math Probl Eng*. 2011;4:480378. [\[CrossRef\]](#)
- [21] Birs I, Muresan C, Nascu I, Ionescu C. A survey of recent advances in fractional order control for time delay systems. *IEEE Access* 2009;7:30951–30965. [\[CrossRef\]](#)
- [22] Chen L, Chai Y, Wu R, Ma T, Zhai H. Dynamic analysis of a class of fractional-order neural networks with delay. *Neural Netw* 2013;111:190–194. [\[CrossRef\]](#)
- [23] Zou G, Wang B. On the study of stochastic fractional-order differential equation systems. *arXiv:1611.07618* 2016. doi: 10.48550/arXiv.1611.07618
- [24] Ross B. Fractional calculus and its applications; Proceedings of the International Conference Held at the University of New Haven, June. Berlin: Springer Verlag; 1974. [\[CrossRef\]](#)
- [25] Samko S, Kilbas A, Marichev O. Fractional integrals and derivatives: theory and applications. Amsterdam: Gordon & Breach Science Publishers; 1993.
- [26] Sher M, Shah K, Sarwar M, Alqudah MA. Mathematical analysis of fractional order alcoholism model. *Alex Eng J* 2023;78:281–291. [\[CrossRef\]](#)
- [27] Khalil R, Horani MA, Yousef A, Sababheh M. A new definition of fractional derivative. *J Comput Appl Math* 2014;264:65–70. [\[CrossRef\]](#)
- [28] Podlubny I. Fractional differential equations. Mathematics in science and engineering. New York: Academic Press; 1999.
- [29] Abdeljawad T. On conformable fractional calculus. *J Comput Appl Math*. 2015;279:57–66. [\[CrossRef\]](#)
- [30] Mostafa E, Rezazadeh H. The first integral method for Wu–Zhang system with conformable time-fractional derivative. *Calcolo* 2015;53:1–11. [\[CrossRef\]](#)
- [31] Chung WS. Fractional Newton mechanics with conformable fractional derivative. *J Comput Appl Math* 2015;290:150–158. [\[CrossRef\]](#)
- [32] Ünal E, Gökdoğan A. Solution of conformable fractional ordinary differential equations via differential transform method. *Optik* 2017;128:264–273. [\[CrossRef\]](#)
- [33] Shehzada K, Ullah A, Saifullah S, Akgül A. Fractional generalized perturbed KdV equation with a power law kernel: a computational study. *Res Control Optim* 2023;12:100298. [\[CrossRef\]](#)
- [34] Ahmad S, Saifullah S. Analysis of the seventh-order Caputo fractional KdV equation: applications to the Sawada–Kotera–Ito and Lax equations. *Commun Theor Phys* 2023;75:085002. [\[CrossRef\]](#)
- [35] Li B, Zhang T, Zhang C. Investigation of financial bubble mathematical model under fractal–fractional Caputo derivative. *Fractals* 2023;31:2350050. [\[CrossRef\]](#)
- [36] Li B, Eskandari Z. Dynamical analysis of a discrete-time SIR epidemic model. *J Frank Inst* 2023;360:7989–8007. [\[CrossRef\]](#)
- [37] He Q, Rahman M, Xie C. Information overflow between monetary policy transparency and inflation expectations using multivariate stochastic volatility models. *Appl Math Sci Eng* 2023;31:2253968. [\[CrossRef\]](#)
- [38] Zhu X, Xia P, He Q, Ni Z, Ni L. Coke price prediction approach based on dense GRU and opposition-based learning salp swarm algorithm. *Int J Bio Inspired Comput* 2023;21:106–121. [\[CrossRef\]](#)
- [39] Hanert E. A comparison of three Eulerian numerical methods for fractional-order transport models. *Environ Fluid Mech* 2010;10:7–20. [\[CrossRef\]](#)
- [40] Khan H, Alzabut J, Shah A, He ZY, Etemad S, Rezapour S, et al. On fractal fractional waterborne disease model: a study on theoretical and numerical aspects of solutions via simulations. *Fractals* 2023;31:2340055. [\[CrossRef\]](#)
- [41] Khan A, Gomez-Aguilar JF, Khan TS, Khan H. Stability analysis and numerical solutions of fractional order HIV/AIDS model. *Chaos Solitons Fractals* 2019;122:119–128. [\[CrossRef\]](#)
- [42] Khan H, Alam K, Gulzar H, Etemad S, Rezapour S. A case study of fractal fractional tuberculosis model in China: existence and stability theories along with numerical simulations. *Math Comput Simul* 2022;198:455–473. [\[CrossRef\]](#)
- [43] Nawaz Y, Arif MS, Shatanawi W. A new numerical scheme for time fractional diffusive SEAIR model with non-linear incidence rate: an application to computational biology. *Fractal Fract* 2022;6:78. [\[CrossRef\]](#)
- [44] Sinan M, Leng J, Shah K, Abdeljawad T. Advances in numerical simulation with a clustering method based on K-means algorithm and Adams–Bashforth scheme for fractional order laser chaotic system. *Alex Eng J* 2023;75:165–179. [\[CrossRef\]](#)
- [45] Sinan M, Ali A, Shah K, Assiri TA, Nofal M. Stability analysis and optimal control of COVID-19 pandemic SEIQR fractional mathematical model with harmonic mean type incidence rate and treatment. *Results Phys* 2021;22:103873. [\[CrossRef\]](#)
- [46] Mohammadnezhad V, Eslami M, Rezazadeh H. Stability analysis of linear conformable fractional differential equations system with time delays. *Bol Soc Paran Mat* 2020;38:159–171. [\[CrossRef\]](#)
- [47] Lin W. Global existence theory and chaos control of fractional differential equations. *J Math Anal Appl* 2007;332:709–726. [\[CrossRef\]](#)
- [48] Paul SK, Mishra LN. Stability analysis through the Bielecki metric to nonlinear fractional integral equations of n-product operators. *AIMS Math* 2024;9:7770–7790. [\[CrossRef\]](#)
- [49] Paul SK, Mishra LN, Mishra VN, Baleanu D. Analysis of mixed type nonlinear Volterra–Fredholm integral equations involving the Erdélyi–Kober fractional operator. *J King Saud Univ Sci* 2023;35:102949. [\[CrossRef\]](#)

- [50] Paul SK, Mishra LN. Approximation of solutions through the Fibonacci wavelets and measure of noncompactness to nonlinear Volterra–Fredholm fractional integral equations. *Korean J Math* 2024;32:137–162.
- [51] Merdan M, Anaç H, Kesemen T. The new Sumudu transform iterative method for studying the random component time-fractional Klein–Gordon equation. *Sigma J Eng Nat Sci* 2019;10:343–354.
- [52] Anaç H, Merdan M, Bekiryazıcı Z. Global stability in a pathogen-specific CD8 immune response prediction model. *Sigma J Eng Nat Sci* 2019;10:325–342.
- [53] Şişman Ş, Merdan M. Global stability of susceptible diabetes complication (SDC) model in discrete time. *Sigma J Eng Nat Sci* 2021;39:290–312. [\[CrossRef\]](#)
- [54] Yadav S, Kumar D, Singh J, Baleanu D. Analysis and dynamics of fractional order COVID-19 model with memory effect. *Results Phys* 2021;24:104017. [\[CrossRef\]](#)
- [55] Inokuti M. General use of the Lagrange multiplier in nonlinear mathematical physics. In: Nemat-Nasser S, ed. *Variational method in the mechanics of solids*. Oxford: Pergamon Press; 1978. p. 156–162. [\[CrossRef\]](#)
- [56] He JH. Some asymptotic methods for strongly nonlinear equations. *Int J Mod Phys B* 2006;20:1141–1199. [\[CrossRef\]](#)
- [57] Bildik N. General convergence analysis for the perturbation iteration technique. *Turk J Math Comput Sci* 2017;6:1–9.
- [58] Odibat ZM. A study on the convergence of variational iteration method. *Math Comput Model* 2010;51:1181–1192. [\[CrossRef\]](#)